

# Variable mass diffusion effects on free convection flow past an impulsively started infinite vertical plate

**B Rushi Kumar, R Jayakar and A G Vijay Kumar**

Department of Mathematics, School of Advanced Sciences, VIT University, Vellore-632014, India

E-mail: rushikumar@vit.ac.in

**Abstract.** An exact analysis of the problem of free convection flow of a viscous incompressible chemically reacting fluid past an infinite vertical plate with the flow due to impulsive motion of the plate with Newtonian heating in the presence of thermal radiation and variable mass diffusion is performed. The resulting governing equations were tackled by Laplace transform technique. Finally the effects of pertinent flow parameters such as the radiation parameter, chemical reaction parameter, buoyancy ratio parameter, thermal Grashof number, Schmidt number, Prandtl number and time on the velocity, temperature, concentration and skin friction for both aiding and opposing flows were examined in detail when  $Pr=0.71$ (conducting air) and  $Pr=7.0$ (water).

## 1. Introduction

Free convection boundary layer flow of a viscous incompressible fluid past a moving vertical infinite plate finds applications in several transport processes in both nature and industrial applications. The analysis of such processes particularly important in the design of chemical processing equipment, formulation, and dispersion of fog, distribution of temperature and moisture over agricultural fields, polymer production, and food processing. Soundalgekar [34] first presented a precise solution to treatment for the flow of a viscous incompressible fluid past an impulsively started infinite vertical plate by Laplace transform technique and he observed that more cooling of the plate by free convection currents might cause separation nearby the plate in case there is air. A precise treatment for the situation of free convection flow past an impulsively started infinite vertical plate in the clear presence of heat flux was presented by Soundalgekar and Patil [35]. Free convection flow of a viscous incompressible fluid past an exponentially accelerated infinite vertical plate was studied by Singh and Kumar [32]. Soundalgekar et al. [36] presented a precise treatment for the flow of an incompressible viscous fluid past an impulsively started infinite vertical plate in the clear presence of foreign mass underneath the conditions of variable plate temperature and constant heat flux. The consequences of free convection currents on the flow of an incompressible viscous fluid past a moving vertical infinite porous plate were studied by Perdakis and Takhar [26]. Mass transfer effects on the flow past an exponentially accelerated vertical plate with constant heat flux were investigated by Jha et al. [12]. Das et al. [7] studied the transient free convection flow past an endless vertical plate with periodic temperature variation. Theoretical solution of flow past an impulsively started vertical plate with variable temperature and mass diffusion was presented by Muthucumaraswamy et al. [19]. The investigation work cited above could be the motivation for the current work.

In several engineering applications such as for example nuclear reactor safety, solar collectors, chemical engineering and food processing there are numerous transport processes with mixed after



effects of buoyancy forces from both thermal and mass diffusion in the occurrence of the chemical reaction. The existence of pure air or water in nature is impossible, and some foreign mass might be present either naturally or combined with them. Furthermore, the clear presence of a foreign mass in air or water causes some sort of chemical reaction. This mass might be appearing either on its own or as mixtures in them. A wide range of research work has been reported in this field. Particularly the analysis of heat and mass transfer with chemical reaction is of significant importance in chemical technologies as well in hydrometallurgical industries. Chamber and Young [4] investigated the consequences of first order chemical reaction in a laminar boundary layer flow in the neighbourhood of a horizontal plate. The combined buoyancy effects in the clear presence of a foreign mass on a totally free convection flow past a semi-infinite vertical plate were studied by Gebhart and Pera [10]. The effect of chemical reaction on heat and mass transfer in laminar boundary-layer flow was investigated by Apelblat [2]. A precise treatment for the flow because of impulsive motion of an infinite vertical plate in the clear presence of i) species concentration ii) constant heat flux iii) chemical reaction was presented by Dass [7], Deka, and Soundalgekar ([8],[9]). The resulting governing equations were tackled by Laplace transform technique. Chamkha et al. [5] studied the consequences of radiation on the free convection flow past a semi-infinite vertical plate in the clear presence of low-level chemical species concentration. Muthucumaraswamy and Ganesan [20] studied the consequences of chemical reaction on a stream past an impulsively started infinite vertical plate with constant heat and mass flux. A theoretical study is conducted to investigate the consequence of chemical reaction on a straight oscillating plate with variable temperature was studied by Muthucumaraswamy and Meenakshisundaram [21]. Again Muthucumaraswamy [22] analyzed the consequences of chemical reaction on a straight oscillating plate with variable temperature. Effect of chemical reaction on free convection flow via a porous medium bounded by a straight surface was studied by Mahapatra et al. [16]. Rajesh and Varma [27] considered the effect of chemical reaction on a totally free convection flow past an exponentially accelerated vertical plate with variable temperature and mass diffusion. Again, Rajesh investigated mass transfer effects on MHD free convection flow with i) variable temperature ii) ramped wall temperature in the clear presence of first order chemical reaction. Unsteady convection with chemical reaction and radiative heat transfer past a flat porous plate moving via a binary mixture in an optically thin environment is studied by Makinde et al [18]. Ibrahim and Makinde [11] investigated the consequences of radiation on chemically reacting MHD boundary layer flow with heat and mass transfer via a porous vertical flat plate in the clear presence of a transverse magnetic field. Again, Makinde [19] also carried out a numerical analysis to examine the combined effects of thermal radiation absorption and magnetic field on an unsteady chemically reacting convective flow past a straight plate in the clear presence of a consistent wall heat flux. Kumar and Varma [38] investigated the consequences of radiation on unsteady MHD flow past an impulsively started exponentially accelerated vertical plate with variable temperature in the clear presence of heat generation. Kumar et al [37] studied the chemical reaction and radiation effects on MHD free convection flow past an exponentially accelerated vertical plate with variable temperature and mass diffusion. Recently, Nandkeolyar et al. [23] considered an unsteady hydromagnetic natural convection flow of a dusty fluid past a moving vertical plate with ramped temperature in the clear presence of thermal radiation.

In most of the studies cited above, the flow is driven either by way of a prescribed surface temperature or even a prescribed surface heat flux. Here, a relatively different driving mechanism for unsteady free convection along a straight surface is known as in this, it's assumed that the flow is because of Newtonian heating from the surface. Heat transfer characteristics are influenced by the thermal boundary conditions. Generally speaking, you can find four classes of heating processes specifying the wall-to-ambient temperature distributions, prescribed surface heat flux distributions, and conjugate conditions, where heat transfer via a bounding surface of finite thickness and finite heat capacity is specified and the interface temperature is unknown a priori but is dependent upon the intrinsic properties of the device, namely, the thermal conductivities of the fluid and solid. In Newtonian heating, the rate of which heat transfers from the bounding surface with a finite heat

capacity is proportional to the neighborhood surface temperature, namely conjugate convective flow. It occurs in several important engineering devices, for instance

(a) in heat exchangers, where conduction in the solid tube wall is greatly influenced by convection in the fluid flowing past it;

(b) in conjugate heat transfer around fins, where conduction within the fin and convection in the fluid surrounding it should be simultaneously analyzed to be able to obtain the vital design information;

(c) in convection flow setups, wherein fact the bounding surfaces absorb the heat of solar radiation.

Therefore, we conclude that the traditional assumption in the lack of interrelation between conduction-convection effects when coupled is not necessarily realistic, and this interaction must certainly be considered while evaluating conjugate heat transfer processes in several practical engineering applications. Merkin [18] was the first to ever look at the free convection boundary layer over a straight flat plate immersed in a viscous fluid. Further, the works of the authors Lesnic et.al ([13], [14], [15]) considered free convection boundary layer flow for the cases of vertical and horizontal surfaces embedded in a porous medium. A precise solution of the unsteady free-convection boundary-layer flow of an incompressible fluid past an endless vertical plate in the clear presence of Newtonian heating was presented by Chaudhary and Jain [6]. Makinde and Chinyoka [17] performed a numerical study to investigate the transient heat transfer in channel flow of an electrically conducting variable viscosity Boussinesq fluid in the clear presence of magnetic field and thermal radiation. Narahari and Ishak [24] investigated the influence of radiation on the unsteady free convection flow of a viscous incompressible fluid past a moving vertical plate with Newtonian heating. Free convection near an impulsively started infinite vertical plate with Newtonian heating in the clear presence of thermal radiation and uniform mass diffusion was studied by Narahari and Nayan [25]. Rajesh [30] presented a precise treatment for the situation of the unsteady free convection flow of a viscous incompressible fluid past an endless vertical plate with Newtonian heating in the clear presence of chemical reaction and uniform mass diffusion.

In this paper, a precise treatment for the situation of unsteady free convection boundary layer flow of a viscous incompressible chemically reacting fluid past an impulsively started infinite vertical plate with Newtonian heating in the clear presence of thermal radiation and variable mass diffusion is investigated using Laplace transform technique. The solutions are obtained with regards to exponential and complementary error functions. The literature concerning this subject is found in books by Carslaw and Jaeger [3] and Slattery [33].

## 2. Mathematical analysis

In this document, we consider an unsteady free convection flow of a viscous incompressible chemically reacting fluid past an impulsively started infinite vertical plate with Newtonian heating in the clear presence of radiation and variable mass diffusion. The  $x'$ -axis is taken over the plate in the vertically upward direction and  $y'$ -axis is taken normal to it. Initially, for a time  $t' \leq 0$  the plate and adjacent fluid are at exactly the same temperature  $T'_\infty$  and concentration  $C'_\infty$  in the whole flow region for the points. At the time  $t' > 0$  the plate is driven having an impulsive motion in the vertically upward direction against to the gravitational field such that it attains characteristic velocity  $u_0$  and at the same time frame the concentration nearby the plate rise linearly by  $t$ . It is assumed that the rate of heat transfer from the top is proportional to the neighbourhood surface temperature  $T'$ . It can be assumed that there exists first-order chemical reaction involving the fluid and species concentration. Considering that the plate is recognized as infinite in the  $x'$ -direction all physical variables are independent of  $x'$  and are functions of  $y'$  and  $t'$  only. After neglecting the consequences of viscous dissipation, Soret and Dufour effects with the most common Boussinesq approximation, the flow

could be proven to be governed by the following system of coupled linear partial differential equations.

$$\frac{\partial u'}{\partial t'} = g\beta(T' - T'_\infty) + g\beta^*(C' - C'_\infty) + \nu \frac{\partial^2 u'}{\partial y'^2} \quad (1)$$

$$\rho c_p \frac{\partial T'}{\partial t'} = \kappa \frac{\partial^2 T'}{\partial y'^2} - \frac{\partial q_r}{\partial y'} \quad (2)$$

$$\frac{\partial C'}{\partial t'} = D \frac{\partial^2 C'}{\partial y'^2} - K_r(C' - C'_\infty) \quad (3)$$

With the initial and boundary conditions

$$\begin{aligned} t' \leq 0: u' = 0, \quad T' = T'_\infty, \quad C' = C'_\infty, \quad \text{for all } y' \\ t' > 0: u' = U_0, \quad \frac{\partial T'}{\partial y'} = -\frac{h}{\kappa} T', \quad C' = C'_\infty + (C'_w - C'_\infty) A t' \quad \text{at } y' = 0 \\ u' = 0, \quad T' \rightarrow T'_\infty, \quad C' \rightarrow C'_\infty \quad \text{as } y' \rightarrow \infty \end{aligned} \quad (4)$$

$$\text{where } A = \frac{U_0^2}{\nu}.$$

The radiative heat flux term is simplified by making use of Rosseland approximation (Siegel and Howell [31]) as:

$$q_r = -\frac{4\sigma}{3K_R} \frac{\partial T'^4}{\partial y'} \quad (5)$$

It should be noted that by using Rosseland approximation, we limit our analysis to optically thick fluids. It is assumed that the temperature differences within the flow are sufficiently small and that  $T'^4$  may be expressed as a linear function of the temperature. This is obtained by expanding  $T'^4$  in a Taylor series about  $T'_\infty$  and neglecting the higher order terms, thus we get

$$T'^4 \cong 4T'^3_\infty T' - 3T'^4_\infty \quad (6)$$

From equations (5) and (6), equation (2) reduces to

$$\rho c_p \frac{\partial T'}{\partial t'} = \kappa \frac{\partial^2 T'}{\partial y'^2} + \frac{16\sigma T'^3_\infty}{3K_R} \frac{\partial T'}{\partial y'^2} \quad (7)$$

All of the physical quantities are defined in the Nomenclature. By introducing the following non-dimensional quantities:

$$\begin{aligned} y = \frac{y' U_0}{\nu}, \quad t = \frac{t' U_0^2}{\nu}, \quad u = \frac{u'}{U_0 Gr}, \quad \theta = \frac{T' - T'_\infty}{T'_\infty}, \quad \text{Pr} = \frac{\mu c_p}{\kappa}, \quad Gr = \frac{\nu g \beta T'_\infty}{U_0^3}, \quad R = \frac{\kappa K_R}{4\sigma T'^3_\infty}, \\ Sc = \frac{\nu}{D}, \quad Gm = \frac{g \beta^* \nu (C'_w - C'_\infty)}{U_0^3}, \quad C = \frac{C' - C'_\infty}{C'_w - C'_\infty}, \quad N = \frac{Gm}{Gr}, \quad K = \frac{K_r \nu}{U_0^3} \end{aligned} \quad (8)$$

The governing system of equations (1), (7) and (3) with the use of (8) is reduced to the following non-dimensional form:

$$\frac{\partial u}{\partial t} = \theta + N C + \frac{\partial^2 u}{\partial y^2} \quad (9)$$

$$3R \text{Pr} \frac{\partial \theta}{\partial t} = (3R + 4) \frac{\partial^2 \theta}{\partial y^2} \quad (10)$$

$$\frac{\partial C}{\partial t} = \frac{1}{Sc} \frac{\partial^2 C}{\partial y^2} - KC \quad (11)$$

The corresponding initial and boundary conditions in dimensionless form become:

$$t \leq 0: u = 0, \theta = 0, C = 0 \text{ for all } y$$

$$t > 0: u = \frac{1}{Gr}, \frac{\partial \theta}{\partial y} = -(1 + \theta), C = t \text{ at } y = 0$$

$$u = 0, \theta \rightarrow 0, C \rightarrow 0 \text{ as } y \rightarrow \infty \quad (12)$$

The coupled linear partial differential Eqs.(9-11) are solved subject to the initial and boundary conditions of Eq.(12) by the usual Laplace transform technique (Abramowitz and Stegun [1]) and the solutions are given in terms of exponential and complementary error functions as follows:

$$C(y, t) = \left[ \left( \frac{t}{2} + \frac{y\sqrt{Sc}}{4\sqrt{K}} \right) \exp(y\sqrt{KSc}) \operatorname{erfc} \left( \frac{y\sqrt{Sc}}{2\sqrt{t}} + \sqrt{Kt} \right) + \left( \frac{t}{2} - \frac{y\sqrt{Sc}}{4\sqrt{K}} \right) \exp(-y\sqrt{KSc}) \operatorname{erfc} \left( \frac{y\sqrt{Sc}}{2\sqrt{t}} - \sqrt{Kt} \right) \right] \quad (13)$$

$$\theta(y, t) = \exp \left( -y + \frac{t}{A} \right) \operatorname{erfc} \left( \frac{y\sqrt{A}}{2\sqrt{t}} - \sqrt{\frac{t}{A}} \right) - \operatorname{erfc} \left( \frac{y\sqrt{A}}{2\sqrt{t}} \right) \quad (14)$$

$$\begin{aligned} u(y, t) = & \left( \frac{1}{Gr} - \frac{N(Sc-1)}{K^2 Sc^2} \right) \operatorname{erfc} \left( \frac{y}{2\sqrt{t}} \right) \\ & + \frac{1}{A-1} \left[ A \exp \left( -\frac{y}{\sqrt{A}} + \frac{t}{A} \right) \operatorname{erfc} \left( \frac{y}{2\sqrt{t}} - \sqrt{\frac{t}{A}} \right) + \left( y\sqrt{A} - A - t - \frac{y^2}{2} \right) \operatorname{erfc} \left( \frac{y}{2\sqrt{t}} \right) + (y - 2\sqrt{A}) \sqrt{\frac{t}{\pi}} \exp \left( -\frac{y^2}{4t} \right) \right] \\ & + \frac{N}{KSc} \left[ \left( t + \frac{y^2}{2} \right) \operatorname{erfc} \left( \frac{y}{2\sqrt{t}} \right) - y \sqrt{\frac{t}{\pi}} \exp \left( -\frac{y^2}{4t} \right) \right] \\ & + \frac{N(Sc-1)}{2K^2 Sc^2} \exp(-bt) \left[ \exp(y\sqrt{-b}) \operatorname{erfc} \left( \frac{y}{2\sqrt{t}} + \sqrt{-bt} \right) + \exp(-y\sqrt{-b}) \operatorname{erfc} \left( \frac{y}{2\sqrt{t}} - \sqrt{-bt} \right) \right] \\ & - \frac{1}{A-1} \left[ A \exp \left( -y + \frac{t}{A} \right) \operatorname{erfc} \left( \frac{y\sqrt{A}}{2\sqrt{t}} - \sqrt{\frac{t}{A}} \right) + \left( (y-1)A - t - \frac{y^2 A}{2} \right) \operatorname{erfc} \left( \frac{y\sqrt{A}}{2\sqrt{t}} \right) + (y-2) \sqrt{\frac{tA}{\pi}} \exp \left( -\frac{y^2 A}{4t} \right) \right] \\ & - \frac{N}{KSc} \left[ \left( \frac{t}{2} + \frac{y\sqrt{Sc}}{4\sqrt{K}} \right) \exp(y\sqrt{KSc}) \operatorname{erfc} \left( \frac{y\sqrt{Sc}}{2\sqrt{t}} + \sqrt{Kt} \right) + \left( \frac{t}{2} - \frac{y\sqrt{Sc}}{4\sqrt{K}} \right) \exp(-y\sqrt{KSc}) \operatorname{erfc} \left( \frac{y\sqrt{Sc}}{2\sqrt{t}} - \sqrt{Kt} \right) \right] \\ & + \frac{N(Sc-1)}{2K^2 Sc^2} \left[ \exp(y\sqrt{KSc}) \operatorname{erfc} \left( \frac{y\sqrt{Sc}}{2\sqrt{t}} + \sqrt{Kt} \right) + \exp(-y\sqrt{KSc}) \operatorname{erfc} \left( \frac{y\sqrt{Sc}}{2\sqrt{t}} - \sqrt{Kt} \right) \right] \\ & - \frac{N(Sc-1)}{2K^2 Sc^2} \exp(-bt) \left[ \exp(y\sqrt{(k-b)Sc}) \operatorname{erfc} \left( \frac{y\sqrt{Sc}}{2\sqrt{t}} + \sqrt{(k-b)t} \right) + \exp(-y\sqrt{(k-b)Sc}) \operatorname{erfc} \left( \frac{y\sqrt{Sc}}{2\sqrt{t}} - \sqrt{(k-b)t} \right) \right] \end{aligned} \quad (15)$$

where  $A = \frac{3RPr}{3R+4}$ ,  $b = \frac{KSc}{Sc-1}$ ,  $erfc(x)$  being the complementary error function defined by

$$erfc(x) = 1 - erf(x), \quad erf(x) = \frac{2}{\sqrt{\pi}} \int_0^x \exp(-\xi^2) d\xi$$

### Skin Friction

From the velocity field, it is interesting to study the changes in the skin-friction. It is given in non-dimensional form as:

$$\tau = -\left. \frac{\partial u}{\partial y} \right|_{y=0} \quad (16)$$

From Eqs.(15) and (16) the skin friction is obtained as follows:

$$\begin{aligned} \tau = & \frac{1}{Gr\sqrt{\pi t}} + 2\sqrt{\frac{t}{\pi}} \left[ \frac{1}{\sqrt{A+1}} + \frac{N}{KSc} \right] + \frac{\sqrt{A}}{\sqrt{A+1}} \left[ 1 - \exp\left(\frac{t}{A}\right) \left( 1 + erf\sqrt{\frac{t}{A}} \right) \right] \\ & - \frac{N}{KSc} \left[ \sqrt{\frac{tSc}{\pi}} \exp(-Kt) + \left( t\sqrt{KSc} + \frac{\sqrt{Sc}}{2\sqrt{K}} \right) erf\sqrt{Kt} \right] \\ & + \frac{N(Sc-1)}{K^2Sc^2} \left[ \sqrt{-b} \exp(-bt) erf(\sqrt{-bt}) + \sqrt{KSc} erf\sqrt{Kt} - \exp(-bt) \sqrt{(k-b)Sc} erf\sqrt{(K-b)t} \right] \quad (17) \end{aligned}$$

### 3. Results and Discussion

With a specific end goal to talk about the impact of different stream parameters going into the issue, for example, R (radiation parameter), N (buoyancy ratio parameter), K (chemical reaction parameter), Sc (Schmidt parameter), Gr (thermal Grashof number) and t (time) on the free convection stream, the numerical estimates for the speed field, temperature field and skin friction were registered and are appeared in figures and tables for the instances of both supporting ( $N>0$ ) and restricting ( $N<0$ ) streams. The estimations of Prandtl number (Pr) are taken as 0.71 and 7.0, which physically compares air and water individually. The temperature profiles for various estimations of t and Pr appear in Figure 1. It can be watched that the heat limit layer thickness is the littlest for water (Pr=7.0) when contrasted with air (Pr=0.71) and an electrolytic arrangement (Pr=1.0). This is because of the way that little Prandtl numbers are equal to increments in heat conductivities, and accordingly, heat can diffuse far from the heated surface more quickly than for higher estimations of the Pr. In this way, temperature falls more quickly for water than for air and electrolytic arrangement. At the point when  $t=0.6$  the heat limit layer thickness diminished by 34.70% and 87.36% when Pr changes from 0.71(air) to 1.0 (electrolytic arrangement) and 7.0(water) individually at the plate ( $y=0$ ). It was additionally watched that the heat limit layer increments by 96.67% and 223.37% for air, by 82.87% and 180.13% for an electrolytic arrangement and by 52.57% and 98.58% for water when t increments from 0.2 to 0.4 and 0.6 individually. Temperature profiles for various estimations of radiation parameter R and Pr at  $t=0.2$  appear in Figure 2. It can be seen that the liquid temperature diminishes with an expansion in R. From the figured estimations of the temperature, when Pr=0.71, 1.0 and 7.0 at  $t=0.2$ , it is discovered that, thickness of the heat limit layer diminishes by 45.72% and 50.78% for air, and by 41.90% and 46.84% for electrolytic arrangement and by 31.27% and 35.65% for water when R changes from 1.0 to 5.0 and 10.0, separately, at the plate.

The buoyancy ratio parameter N speaks to the proportion of the mass and heat lightness powers and there are three conceivable cases I)  $N=0$ , there is no mass exchange and the lightness constraint is

because of heat dissemination just ii)  $N > 0$ , the mass lightness drive acts an indistinguishable way from heat lightness compel. iii)  $N < 0$ , the mass lightness drive acts inverse way of the heat lightness constraint. The speed profiles for various estimations of buoyancy ratio parameter  $N$  for both helping and restricting impacts of the mass movements appear in Figure 3 and 4 when  $R=10$ ,  $Gr=2.0$ ,  $Sc=0.6$ ,  $K=0.5$  and  $t=0.6$  for the cases both water and air. It can be unmistakably observed that the speed increments with expanding estimations of  $N$  for both water and air for helping streams. This is the explanation behind the expansive lightness compels caused by the concentration distinction. On account of restricting streams, with an expansion in contradicting lightness constrain the speed diminishes for water and also air. From the ascertained estimations of the speed it is discovered that when  $R=10$ ,  $Gr=2.0$ ,  $Sc=0.6$ ,  $K=0.5$  and  $t=0.6$ , the force limit layer thickness increments by 11.68% , 23.34% and 35% when  $N$  increments from 0 to 2.0, 4.0 and 6.0 for air and by 17.59%, 35.20% and 52.79% for water on account of helping stream, while it diminishes by 11.66%, 23.32% and 35% for air and by 17.59%, 35.17% and 52.79% for water on account of contradicting stream, when  $N$  diminishes from 0 to - 2.0, - 4.0 and - 6.0 separately at  $y=0.3$ .

The speed profiles are plotted in Figure 5 and 6 for various estimations of radiation parameter  $R$  when  $Gr=2.0$ ,  $Sc=0.6$ ,  $K=0.5$  and  $t=0.6$  for both water and air in the instances of helping and contradicting streams. It can be seen that speed diminishes with the expansion of radiation parameter  $R$ . Physically, it meet the rationale that an expansion in the radiation parameter  $R$ , the rate of radiative heat exchanged to the liquid abatements, and thusly the liquid speed diminishes alongside the temperature. What's more, henceforth, there is a fall in the speed with the radiation parameter  $R$ . From the figured estimations of the speed, it is watched that when  $Gr=2.0$ ,  $Sc=0.6$ ,  $K=0.5$  and  $t=0.6$  if there should arise an occurrence of air, the speed diminishes by 43.08% and 46.52% for a supporting stream and by 43.62% and 47.10% for restricting stream when  $R$  increments from 1.0 to 5.0 and 10.0 separately. If there should arise an occurrence of water for a supporting stream when  $R$  increments from 0.1 to 0.5 and 5.0 the speed diminish by 37.44% and 42.51% and by 38.21% and 43.37% for contradicting streams.

The speed disseminations are plotted in Figure 7 and 8 for various estimations of  $Gr$  for the instances of supporting and contradicting streams. It can be seen that an expansion in  $Gr$  prompted a decline in the speed for supporting and in addition contradicting stream. It is discovered that when  $R=10$ ,  $Sc=0.6$ ,  $K=0.5$  and  $t=0.6$  the energy limit layer thickness diminishes by 31.82% and 42.44% for air and by 47.71% and 63.63% for water on account of supporting stream. It is additionally watched that for contradicting streams the force limit layer thickness diminishes by 32.57% and 43.44% for air and by 49.42% and 65.91% for water when  $Gr$  increments from 2.0 to 4.0 and 6.0 at  $y=0.3$ . From Figure 9 and 10 it can be likewise observed that the speed increments as time advanced for air and water in the instances of both helping and contradicting streams. In this way, for  $R=10$ ,  $Gr=2.0$ ,  $Sc=0.6$ ,  $K=0.5$  and  $N=0.2$  (aiding stream), the energy limit layer thickness increments by 29.42% and 68.25% for air and by 8.62% and 15.26% for water when  $t$  increments from 0.4 to 0.6 and 0.8 separately, at  $y=0.3$ , and for  $R=10$ ,  $Gr=2.0$ ,  $Sc=0.6$ ,  $K=0.5$  and  $N=-0.2$  (opposing stream), thickness of the force limit layer increments by 28.32% and 65.83% for air and by 6.84% and 11.21% for water when  $t$  increments from 0.4 to 0.6 and 0.8 individually, at  $y=0.3$ .

The liquid speed for various estimations of Schmidt number  $Sc$  and Prandtl number  $Pr$  are plotted in Figure 11 when  $R=10$ ,  $Gr=2.0$ ,  $K=0.5$ ,  $t=0.6$ , and  $N=0.2$ . It can be seen that the speed diminishes for both air and water because of an expansion in  $Sc$ . An expansion in Schmidt number infers that thick powers overwhelm over the dissemination impacts. Along these lines, there is a diminishing in the speed of air and water because of an expansion in the estimation of the Schmidt number. From the computed estimations of the speed when  $R=10$ ,  $Gr=2.0$ ,  $K=0.5$ ,  $t=0.6$  and  $N=0.2$ , the force limit layer thickness diminishes by 0.77% and 1.16% for air and by 1.15% and 1.72% for water when  $Sc$  increments from 0.01 to 0.22 and 0.60 separately, at  $y=0.3$ . The variety in speed for air and water appear in Table 1 and 2 for various estimations of  $K$  (chemical reaction parameter) when  $R=10$ ,  $Sc=0.6$ ,  $Gr=2.0$  and  $t=0.6$  in the instances of both helping and contradicting streams. It is discovered that there is fall in the speed of air or water because of an expansion in the estimations of substance

response parameter on account of supporting stream, while it increments for restricting streams. It is discovered that when  $K$  expanding from 0.5 to 5 and 10, individually, the force limit layer diminishes by 0.33% and 0.57% for air and by 0.53% and 0.88% for helping streams, though it increments by 0.35% and 0.57% for air and by 0.58% and 0.94% for water if there should be an occurrence of restricting streams at  $y=0.4$ . The fixation profiles for various estimations of Schmidt number ( $Sc$ ), concoction response parameter ( $R$ ) and time  $t$  are exhibited in Figure 12. From this figure, it can be seen that the concentration diminishes with the expansion in  $Sc$  or  $K$ , while it increments with time  $t$ .

The variety of the skin-friction at the plate appears in Table 3 and 4 for unique estimations of the representing parameters. It is watched that the skin erosion diminished as the time advanced for both helping and restricting streams. It can be seen that friction diminishes by 71.91% and 86.18% for air, and by 68.91% and 78.84% for water on account of supporting stream, for restricting streams it diminishes by 71.71% and 85.65% for air and by 68.72% and 78.31% for water, when  $t$  increments from 0.01 to 0.1 and 0.2, separately. As the radiation parameter  $R$  expands erosion at the plate additionally increments for both helping and restricting streams and it is likewise discovered that skin friction increments by 2.44% and 2.72% for air and by 3.96% and 4.47% for water if there should be an occurrence of supporting stream and it increments by 2.14% and 2.37% for air and 3.85% and 4.35% for water if there should arise an occurrence of contradicting stream, when  $R$  increments from 1.0 to 5.0 and 10.0, individually. The skin friction abatements for supporting streams, while it increments for contradicting streams for both air and water. From the computed estimations of the skin erosion, it is watched that friction declines by 1.93% and 3.87% in the event of air and 1.26% and 2.52% if there should arise an occurrence of water for supporting streams when  $N$  increments from 0.2 to 0.4 and 0.6, separately, while it increments by 1.86% and 3.72% in the event of air and 1.22% and 2.46% in the event of water for restricting streams, when  $N$  diminishes from - 0.2 to - 0.4 and - 0.6, individually.

The skin friction expanded with expanding estimations of  $K$  or  $Sc$ , though the friction diminished with the expansion in the estimations of  $Gr$  for both air and water in instances of both supporting and restricting streams. From the figured estimations of skin contact it is discovered that when  $Sc$  increments from 0.6 to 0.78 and 0.96, separately, the skin friction increments by 0.11% and 0.20% for air and by 0.07% and 0.13% for water on account of supporting streams, and the friction is found to diminishes by 0.11% and 0.19% for air and by 0.07% and 0.13% for water on account of contradicting streams. This outcome might be clarified by the way that with an expansion in the estimation of  $Sc$  prompts a lessening in mass buoyancy impact, and subsequently, there is more erosion at the moving plate.

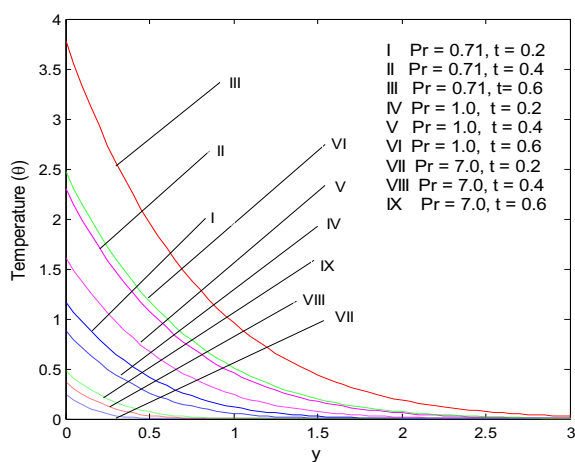


**Figure 1.** Temperature profiles for different  $Pr$  and  $t$  when  $R=10$

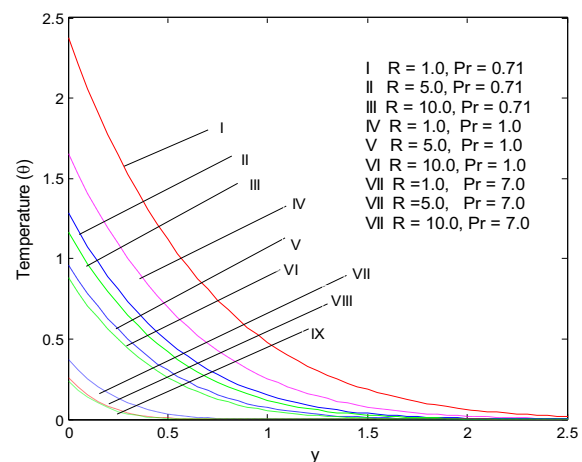


**Figure 2.** Temperature profiles for different  $R$  and  $Pr$  when  $t=0.2$

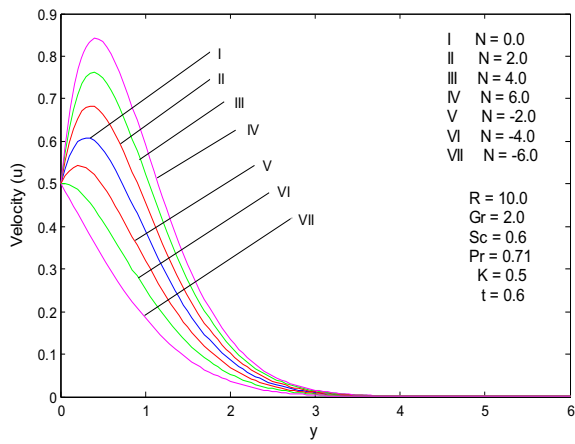


**Figure 3.** Velocity for different N when Pr=0.71

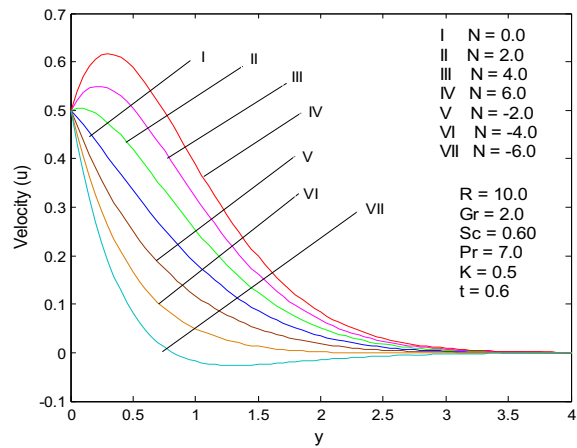


**Figure 4.** Velocity for different N when Pr=7

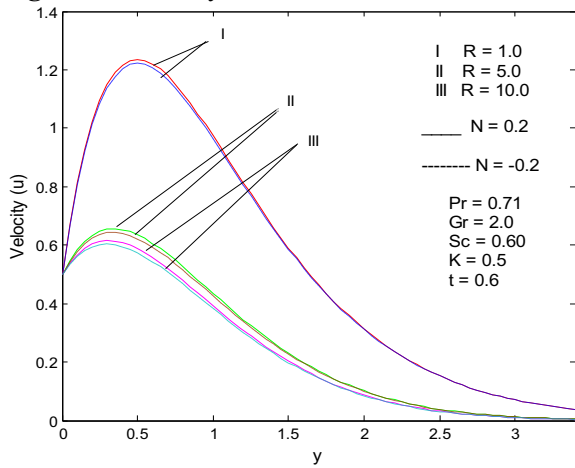


**Figure 5.** Velocity profiles for different R when Pr=0.71

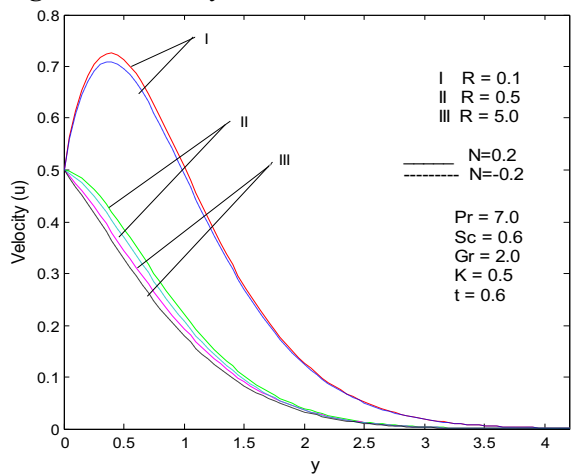


**Figure 6.** Velocity profiles for different R when Pr=7

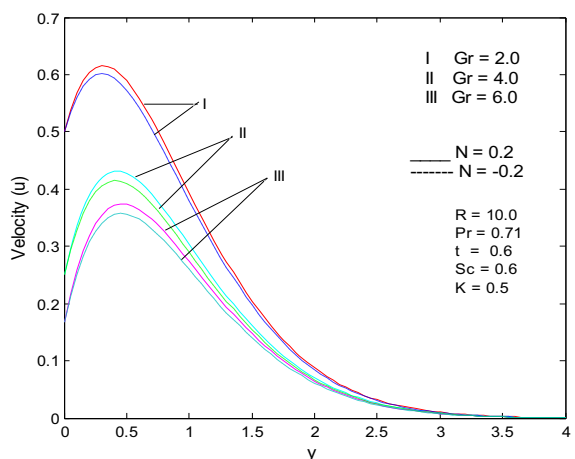


**Figure 7.** Velocity profiles for different Gr when Pr=0.71

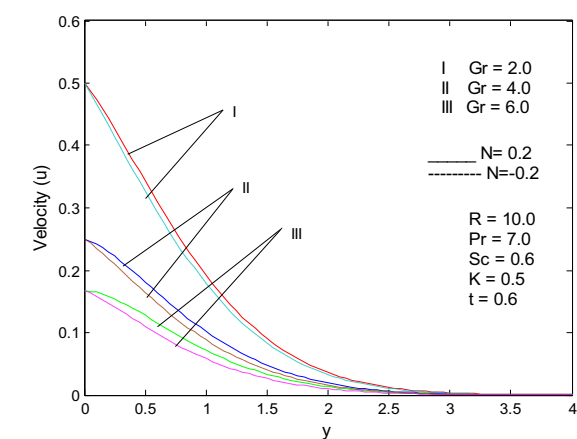


**Figure 8.** Velocity profiles for different Gr when Pr=7.0

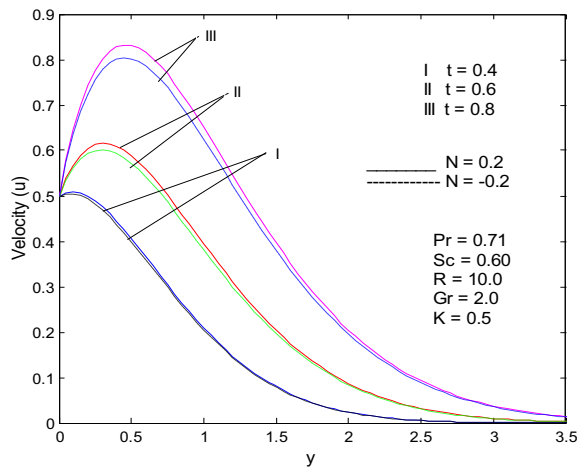


**Figure 9.** Velocity profiles for different t when Pr=0.71

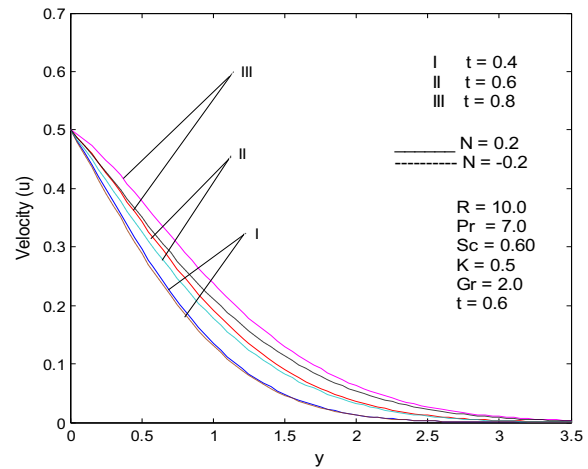


**Figure 10.** Velocity profiles for different t when Pr=7.0

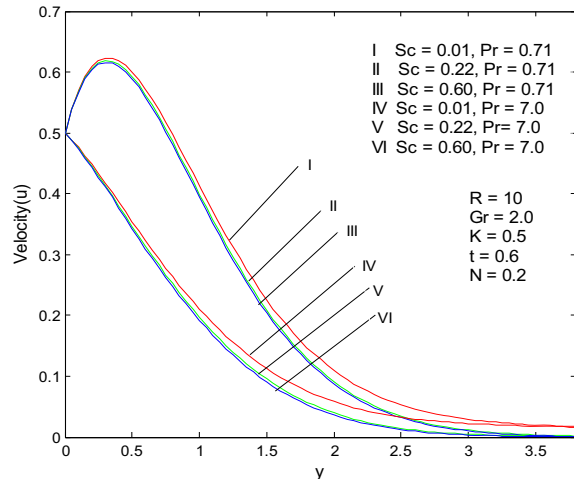


**Figure 11.** Velocity profiles for different Sc and Pr

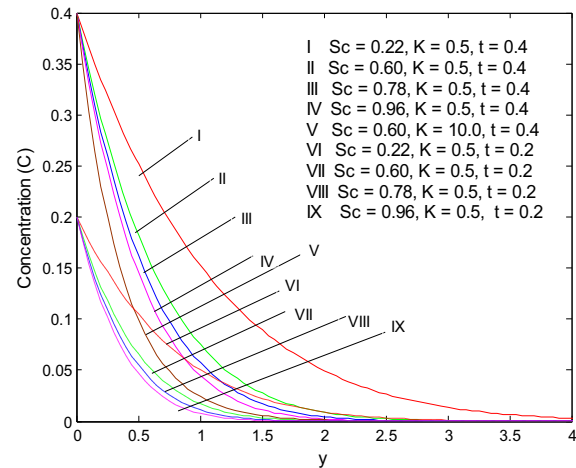


**Figure 12.** Concentration profiles for different Sc, K, and t

#### 4. Conclusions

This work concentrated on the explanatory arrangement of the unsteady free convection heat and mass exchange of an incompressible synthetically responding liquid past a limitless vertical plate with the stream caused by Newtonian heating and indiscreet movement of the plate within the presence of thermal radiation. The governing partial differential conditions were solved with the assistance of Laplace Transform method with no limitations. The impacts of different stream parameters going into the issue on the speed, temperature and concentration fields, and the skin friction were contemplated in detail for both helping and contradicting streams when Pr=0.71(conducting air) and Pr=7.0(water).The following fundamental conclusions can be drawn from the present investigation are:

1. Increase in Pr or R diminishes in the heat limit layer while it increments with an expansion in time t.
2. Temperature falls more quickly for water than air and an electrolytic arrangement.
- 3.The speed of the liquid is lessened, though the skin-rubbing improved as the K or Sc expanded for supporting streams while the skin friction was reduced by restricting streams with an expansion in Sc or K.
4. Momentum and heat limit layer thickness diminish as R increments, though the friction was improved for both helping and restricting streams.

5. Finally, the liquid speed improved, though skin friction was decreased as lightness proportion parameter N is amplified.

## References

- [1] Abramowitz B M and Stegun I A 1970 *Handbook of Mathematical Functions*, Dover Publications, Inc. New York.
- [2] Apelblat A 1982 *Chem. Eng. J.* **23** 193-203
- [3] Carslaw H S and Jaeger J C 1959 *Conduction of Heat in Solids* (2<sup>nd</sup> eds.), Oxford University Press, London.
- [4] Chambre, P.L. and Young, J.D 1958 *Phys. Fluids*, **1** 48-54
- [5] Chamkha A J Takhar H S and Soundalgekar V M 2001 *Chem. Eng. J.* **84** 335-342
- [6] Chaudhary R C and Jain P 2007 *J. Eng. Phys. Thermophy.* **80** 954-960
- [7] Das U N Deka R K and Soundalgekar V M 1999 *J. Heat Transfer*, **121** 1091-1094
- [8] Dass U N Deka R K and Soundalgekar V M 1999 *Bull. GUMA*, **5** 13-20
- [9] Dass U N Deka R K and Soundalgekar V M 1994 *Forschung Im Ingenieurwesen*, **69** 284-287
- [10] Gebhart B and Pera L 1971 *Int. J. Heat Mass Transfer*, **14**(2) 2025-2050
- [11] Ibrahim S Y and Makinde O D 2011 *Int. J. Phy. Sci.* **6**(6) 1508-1516
- [12] Jha B K Prasad R and Rai S 1991 *Astrophys. Space Sci.* **181** 125-134
- [13] Lesnic D Ingham D B and Pop I 1999 *Int. J. Heat Mass Transfer* **42** 2621-2627
- [14] Lesnic D Ingham D B and Pop I 2000 *J. Porous Media* **3** 227-335
- [15] Lesnic D Ingham D B Pop I and Storr C 2003 *Heat Mass Transfer* **40** 665-672
- [16] Mahapatra N Dash G C Panda S and Acharya M 2010 *J. Eng. Phy. and Therm.* **83**(1)
- [17] Makinde O D and Chinyoka T 2010 *Comm. Non. Sci. and Num. Simu.* **15** 3919-3930
- [18] Makinde O D Olanrewaju P O and Charles W M 2011 *Afrika Matematika* **22** 65-78
- [19] Makinde O D 2012 *Zeitschrift für Naturforschung* **67a** 239-247
- [18] Merkin J H 1994 *Int. J. Heat Fluid Flow* **15** 392-398
- [19] Muthucumaraswamy R Ganesan P and Soundalgekar V M 2000 *Forschung Im Ingenieurwesen* **66** 147-151
- [20] Muthucumaraswamy R and Ganesan P 2001 *Acta Mechanica* **147** 45-57
- [21] Muthucumaraswamy R and Meenakshisundaram S 2006 *Theor. Appl. Mech.* **33**(3) 247-257
- [22] Muthucumaraswamy R 2010 *CI&CEQ* **16**(2) 167-173
- [23] Nandkeolyar R Seth G S Makinde O D Sibanda P and Ansari M S 2013 *J. App. Mech.* **80** 061003(1-9)
- [24] Narahari M and Ishak A 2011 *J. App. Sci.*, **11**(7): 1096-1104.
- [25] Narahari M and Yunus Nayan M 2011 *Turkish J. Eng. Env. Sci.* **35** 187-198
- [26] Perdikis C P and Takhar H S 1986 *Astrophys. Space Sci.* **125** 205-209
- [27] Rajesh V and Varma S V K 2010 *Annals-J. Eng., VIII, Fascicule 1* 181-188
- [28] Rajesh V 2010 *Annals-J. Eng., VIII, Fascicule 3* 370-378
- [29] Rajesh V 2010 *Annals-J. Eng., VIII, Fascicule 3* 426-433
- [30] Rajesh V 2011 *J. of Eng. Phys. and Thermophys* **85**(1) 221-228
- [31] Siegel R and Howell J R 2002 *Thermal Radiation Heat Transfer*, 4<sup>th</sup> Edition, Talyor and Francis, New York.
- [32] Singh A K and Kumar N 1984 *Astrophys. Space Sci.* **98** 245-248
- [33] Slattery J C 1999 *Advanced Transport Phenomena*, Cambridge University Press.
- [34] Soundalgekar V M 1977 *J. Heat Transfer*, **99** 499-501
- [35] Soundalgekar V M and Patil M R 1980 *Astrophys. Space Sci.* **70** 179-182
- [36] Soundalgekar V M Birajdar N S and Darwhekar V K 1984 *Astrophys. Space Sci.* **100** 159-164
- [37] Kumar A G Varma S V K and Ram mohan 2012 *Annals-J. Eng. Tome X, Fascicule 2* 195-202
- [38] Kumar A G and Varma S V K 2011 *Int. J. Eng. Sci. and Tech.* **3**(4) 2011